



**HAL**  
open science

# Structural, Electronic, Thermodynamic, Optical and Nonlinear Optical Properties of Curcumin Complexes with Transition Metals: DFT and TD-DFT Study

Ahlem Khireddine, Mebarek Boukelkoul, Yusuf Atalay, Ömer Tamer, Davut Avc , Lynda Merzoud, Henry Chermette

## ► To cite this version:

Ahlem Khireddine, Mebarek Boukelkoul, Yusuf Atalay, Ömer Tamer, Davut Avc , et al.. Structural, Electronic, Thermodynamic, Optical and Nonlinear Optical Properties of Curcumin Complexes with Transition Metals: DFT and TD-DFT Study. *ChemistrySelect*, 2022, 7 (14), 10.1002/slct.202104442 . hal-04279818

**HAL Id: hal-04279818**

**<https://hal.science/hal-04279818>**

Submitted on 10 Nov 2023

**HAL** is a multi-disciplinary open access archive for the deposit and dissemination of scientific research documents, whether they are published or not. The documents may come from teaching and research institutions in France or abroad, or from public or private research centers.

L'archive ouverte pluridisciplinaire **HAL**, est destinée au dépôt et à la diffusion de documents scientifiques de niveau recherche, publiés ou non, émanant des établissements d'enseignement et de recherche français ou étrangers, des laboratoires publics ou privés.

# Structural, Electronic, Thermodynamic, Optical and Nonlinear Optical Properties of Curcumin Complexes with Transition Metals: DFT and TD-DFT Study

Ahlem Khireddine<sup>a</sup>, Mebarek Boukelkoul<sup>b,\*</sup>, Yusuf Atalay<sup>c</sup>, Ömer Tamer<sup>c</sup>, Davut Avci<sup>c</sup>, Lynda Merzoud<sup>d</sup> and Henry Chermette<sup>d,\*</sup>

<sup>a</sup> Laboratoire de Physique Quantique et Systèmes Dynamiques, Chemistry Department, Sciences Faculty, Ferhat Abbas Sétif-1 University, 19000 Sétif, Algeria

<sup>b</sup> Laboratoire de Physique Quantique et Systèmes Dynamiques, Physics Department, Sciences Faculty, Ferhat Abbas Sétif-1 University, 19000 Sétif, Algeria

<sup>c</sup> Sakarya University, Faculty of Arts and Sciences, Department of Physics, 54187, Sakarya, Turkey

<sup>d</sup> Université de Lyon, Université Claude Bernard Lyon 1, Institut des Sciences Analytiques, UMR CNRS 5280, 69622 Villeurbanne Cedex, France

\*Corresponding author. E-mail: henry.chermette@univ-lyon1.fr

## Abstract

Because of their important photonic applications, the curcumin molecules, which can easily be found in nature, are interesting in the study of nonlinear optical (NLO) properties. Density functional theory (DFT) calculations on ground state molecular geometries of [(bpy-CH<sub>3</sub>)M(curc)] Cl complexes, where M = Cr, Mn, Fe, Co, Ni, Cu, Zn, Mo, Tc, Ru, Rh, Pd, Ag, Cd, W, Re, Os, Ir, Pt, Au and Hg, have been performed at B3LYP level. Most complexes have a pyramidal geometry with square base, with a few exceptions well understood from the electronic structure of the metal atom. Although the pyramid geometry with square base of the [(bpy-CH<sub>3</sub>)Zn(curc)] Cl complex is preserved in solution, our DFT calculations show that the Zn lying above the square plane becomes closer and closer to that plane when the solvent is more and more polar, whereas the dipole moment increases in the mean time. The calculated IR spectra for the Zn complex show an increase in the intensity of the peaks of solvated complexes. The effect of solvent on excitation transition types and electronic spectra of the transition metal complexes simulated using DFT-CPCM model shows intra-ligand charge transfer from HOMO to LUMO in polar solvents, but from HOMO to LUMO+1 in apolar solvents. Among a full set of properties of transition metal series complexes with 21 elements, it appears that the Mn, Ag and Re complexes are the best candidates to NLO materials.

1  
2  
3  
4  
5  
6  
7  
8  
9  
10  
11  
12  
13  
14  
15  
16  
17  
18  
19  
20  
21  
22  
23  
24  
25  
26  
27  
28  
29  
30  
31  
32  
33  
34  
35  
36  
37  
38  
39  
40  
41  
42  
43  
44  
45  
46  
47  
48  
49  
50  
51  
52  
53  
54  
55  
56  
57  
58  
59  
60  
61  
62  
63  
64  
65

Finally, an excellent correlation between the magnetic moments per atom and the number of valence electron of the central metals is obtained.

## Introduction

During the past few decades, a wide number of works have been achieved and published for materials with remarkable Nonlinear Optical (NLO) properties.<sup>[1-4]</sup> This interest is due to their technological potentials as well as their vast applications in various domains such as electro-optic (EO) switches and modulators,<sup>[5,6]</sup> the generation of ultrashort laser pulses, telecommunications and signal processing,<sup>[7,8]</sup> optical devices<sup>[9-11]</sup> and other potential applications.<sup>[12-17]</sup> Numerous organic NLO materials are excellent candidates for study, hence their increased attraction and special attention given by researchers following their outstanding advantages in relation to classic inorganic materials. Such advantages are, for instance, a small cost of production, low absorption loss, easiness when adjusting and manipulating, decreased dielectric constants and increased photoelectric coefficients.<sup>[18-22]</sup>

Curcumin, derived from the dried rhizome of *curcuma longa* L is famous for its diverse applications in cosmetics and pharmaceuticals, and its yellow orange pigment is well known. On the other hand, turmeric (*Curcuma Longa*) is an Indian spice present in Ayurveda, an inflammatory medicine known by different names in several cultures. The active principle is surnamed curcumin or diferuloylmethane.<sup>[23]</sup> Curcumin[1,7-bis (4-hydroxy-3-methoxy phenyl)-1,6-hepta-diene-3,5-dione] has drawn much attention recently, probably because of its wide uses in biological, pharmaceuticals and cosmetics, which include antiviral, antibacterial, anticoagulant activities, antifungal,<sup>[24]</sup> antioxidant,<sup>[25]</sup> anti-inflammatory<sup>[26]</sup> and antitumor.<sup>[23]</sup>

In addition to this, curcumin molecules have important photonic applications.<sup>[27,28]</sup> They are very interesting in the study of nonlinear optical (NLO) properties considering that they can easily be found in nature. Organic materials have accentuated its importance recently in the field of optical data storage, telecommunications optical signal processing,<sup>[29]</sup> because they possess a purely electrical origin of polarizability, coupled with large first hyperpolarizability ( $\beta$ ) with respect to inorganic materials. In the course of development of second order organic NLO materials, D- $\pi$ -A molecules, that are  $\pi$ -conjugate systems attached by a donor (D) and acceptor (A) group, are the first choice.<sup>[30-32]</sup> Excellent linear and nonlinear optical characteristics of these chromophores and the relative orientation of donor and acceptor cores ameliorate their

1 first hyperpolarizability ( $\beta$ ) values.<sup>[33,34]</sup> It is customary to experimentally measure NLO  
2 properties through hyper-Rayleigh scattering (HRS) in the near infrared, and electric-field  
3 induced second harmonic generation (EFISHG), with femtosecond laser pulses.<sup>[35,36]</sup>  
4  
5

6 Theoretical research and studies of coordination and organometallic compounds are essential  
7 to understand the structure and dynamics of electronic excited states in photochemistry,  
8 photophysics, and spectroscopy.<sup>[37,38]</sup> By virtue of their rich excited-state behavior and  
9 fundamental importance, these researches are pushed more and more by applications of  
10 transition metals (TM) complexes as luminescence based sensors, nonlinear optical materials,  
11 organic lightemitting diodes (OLED), photoinitiators, molecular devices (moletronics),  
12 photocatalysts, solar energy conversions, or triggers of electron transfer in biomolecules.  
13  
14  
15  
16  
17  
18  
19

20 Presently, density functional theory (DFT) and time dependent DFT (TD-DFT) are becoming  
21 the most advanced tools for the understanding of photophysical properties of organic molecules.  
22 The present study concentrates on DFT calculations of complexes of curcumin [(bpy-  
23 R)M(curc)] Cl where M=Zn and R=C<sub>9</sub>H<sub>19</sub>, developed by Pucci et al.<sup>[39]</sup> The computational  
24 study is achieved in order to fathom the effect of the nature of TMs on geometries, electronic  
25 parameters, magnetic moment, thermodynamic characteristics, optical and NLO properties,  
26 aside from finding a correlation between these parameters.  
27  
28  
29  
30  
31  
32

33 This paper is organized as follow: After a description of the computational details applied to  
34 the experimental molecular structure of the Zn complex, the results are analyzed and then  
35 discussed in detail. The final Section presents our conclusion.  
36  
37  
38  
39

## 40 **Computational Methods**

41

42 Starting from the X-ray crystallographic molecular structure of the [(bpy-R)M(curc)] Cl where  
43 M= Zn and R=C<sub>9</sub>H<sub>19</sub>, are reported by Pucci and co-workers<sup>[39,40]</sup> The calculations have been  
44 performed using Gaussian09,<sup>[41]</sup> where the R is replaced by CH<sub>3</sub> and M = Cr, Mn, Fe, Co, Ni,  
45 Cu, Zn, Mo, Tc, Ru, Rh, Pd, Ag, Cd, W, Re, Os, Ir, Pt, Au and Hg. The DFT method at B3LYP  
46 level and LANL2DZ basis set is used to obtain optimized molecular structure of [(bpy-  
47 R)M(curc)] Cl complexes in the ground state and to calculate thermodynamic parameters, with  
48 no symmetry restrictions. All the optimized structures have been obtained with no imaginary  
49 frequencies through harmonic vibrational frequency calculations. The 0.9614 scaling factor has  
50 been applied to the obtained vibration frequencies, in order to roughly reduce the well know  
51 difference between B3LYP harmonic vibration frequencies and anharmonic experimental  
52  
53  
54  
55  
56  
57  
58  
59  
60  
61  
62  
63  
64  
65

ones.<sup>[42,43]</sup> Starting from the ground-state geometry and in different solvents phase, the optimized structures, the harmonic vibrational frequencies and the molecular orbital spectra have been calculated, as well as the electronic optical spectra by using the time-dependent DFT (TD-DFT) method. Besides, the conductor-like-polarizable continuum model (CPCM)<sup>[44-46]</sup> has also been used to consider solvent effects. Finally, the linear and nonlinear optical properties of [(bpy-R)M(curc)] Cl complexes have also been investigated by the calculation of dipole moment ( $\mu$ ), polarizability ( $\alpha$ ), anisotropy of polarizability ( $\Delta\alpha$ ) and first hyperpolarizability( $\beta$ ).

## Results and discussion

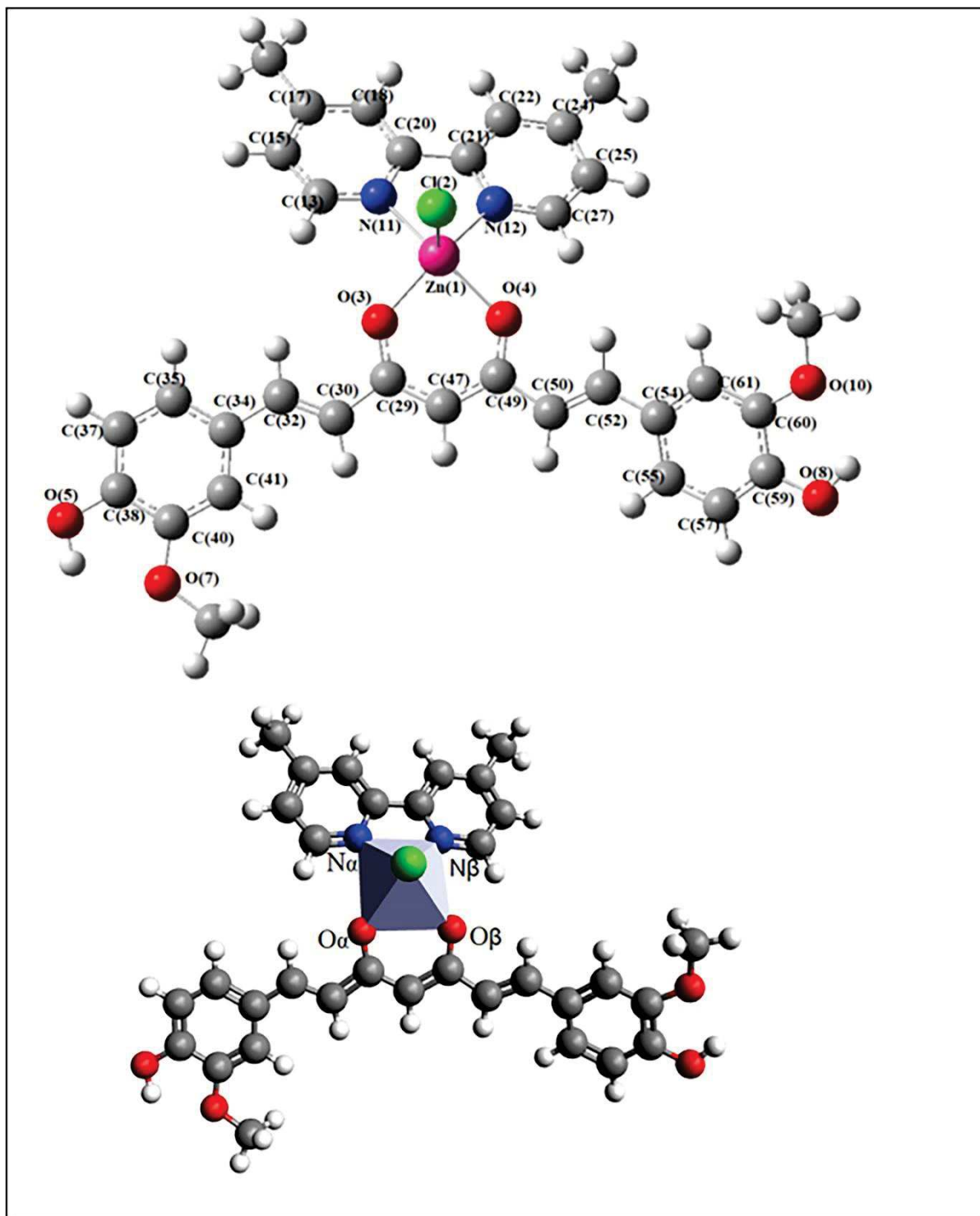
### Structural analyses

The molecular structure of the Zn(II) complex with the atom labels and ground state geometry optimized by B3LYP level is presented in Scheme 1. The experimental and theoretical interatomic distances and angles are gathered in Table S-1.

As shown in Scheme 1, the [(bpy-CH<sub>3</sub>)Zn(curc)] Cl complex has a pyramidal geometry with a square base, the chlorine atom located at the top of the pyramid and the basal plane is formed by 2 oxygen and 2 nitrogen. Some calculated bond lengths and angles of the complex, are compared to their experimental counterparts. The distance between Zn and the centroid of the NNOO atoms basal plane is equal to 0.697 Å and it is very comparable to the experimental results.<sup>[39]</sup> The experimental bond lengths of M-O $\alpha$  and M-O $\beta$  were observed respectively at 2.015 Å and 2.030 Å for M = Zn,<sup>[39]</sup> 2.083 Å and 2.073 Å for M = Rh,<sup>[47]</sup> 1.917 Å and 1.934 Å for M = Cu.<sup>[48]</sup> These bond lengths are calculated as 2.046 Å and 2.057 Å, 2.056 Å and 2.057 Å, 1.947 Å and 2.114 Å, respectively for M = Zn, Rh, Cu.

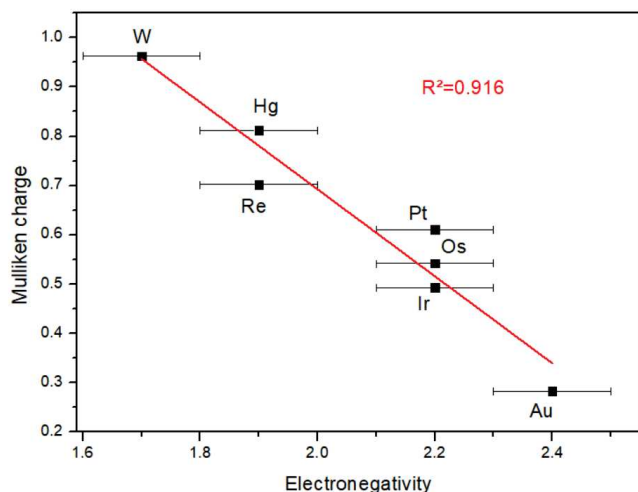
The M-Cl bond length experimentally amounting 2.292 Å for M = Zn and 2.463 Å for M = Rh is calculated at 2.348 Å and 2.597 Å, respectively.

The bond angles of N $\alpha$ -Zn-N $\beta$ , O $\alpha$ -Zn-O $\beta$ , N $\alpha$ -Zn-O $\alpha$  and N $\beta$ -Zn-O $\beta$  which are experimentally found at 76 deg, 99 deg., 86 deg. and 91 deg., respectively, are calculated at 74 deg., 88 deg., 88 deg. and 88 deg.. The largest bond angle O $\alpha$ -Zn-O $\beta$  was experimentally observed at 150 deg., and the bond angle of O $\beta$ -M-N $\alpha$  is calculated at 152 deg.. The torsion angle N $\alpha$ -N $\beta$ -O $\beta$ -O $\alpha$  found experimentally at -2 deg. is theoretically calculated at 15 deg.. These results indicate that this level of theory lets reproduce satisfactorily the experimental results.



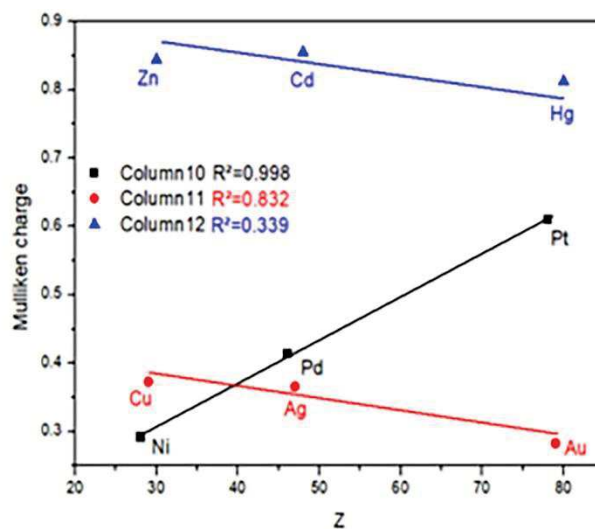
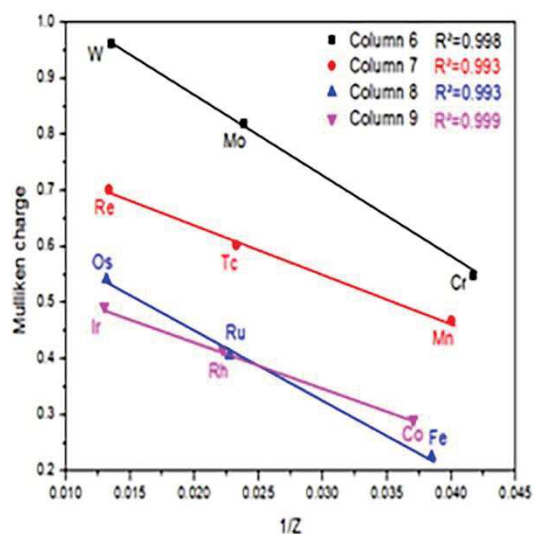
**Scheme 1.** Geometry and structure with atomic numbering of [(bpy-R)Zn(cure)]Cl complex.

Figure 1 shows an excellent linear correlation between Mulliken charge and Pauling electronegativity<sup>[49,50]</sup> with  $R^2 = 0.916$  for the third row transition metals.



**Figure 1.** The correlation between Mulliken charge and electronegativity of the central metal of [(bpy-CH<sub>3</sub>)M(curc)]Cl complexes, with a margin of error  $\pm 0.1$  on electronegativity.

As shown in Figure 2, Mulliken charges vary linearly with the inverse of the atomic number  $Z$  for the first four columns starting from column 6 (which contains Cr, Mo and W) up to the column 9. This indicates that when  $Z$  increases within a column, the metal-ligand bond becomes more ionic, whereas, within a row, the ionicity decreases. On the other hand, a good linear correlation with the atomic number  $Z$  is obtained for the column 10 (Ni, Pd and Pt) with  $R^2 = 0.998$ . For the last two columns, there is no correlation, one reason being that the corresponding complexes differ in geometry and possess the largest values of the dipole moment when compared to the values of the elements of the previous columns. Let us recall that the elements of the 11th and 12th column of the periodic table have a saturated d valence shell, being so-called complexes with 19 and 20 electrons, a well-known feature of weak stability.<sup>[51]</sup>



**Figure 2.** The correlation between Mulliken charge and the atomic number of the central metal of [(bpy-CH<sub>3</sub>)M(curc)]Cl complexes.

There is a global trend of increase of the dipole moment with respect to the atomic number of the central metal of [(bpy-CH<sub>3</sub>)M(curc)]Cl complexes: Indeed a good correlation between dipole moment and atomic number can be observed for 4d and 5d elements (Figure 3), Au excepted. This is less true for 3d elements, even when excluding Cu from the correlation. This may be connected to the propensity of the elements from the middle of the 4th row (3d) to make (magnetic) complexes of different spin states. As is well known, Au and Cu exhibit a propensity to prefer monovalency in complexes. Besides, these atoms from column 11 are among the most electronegative.

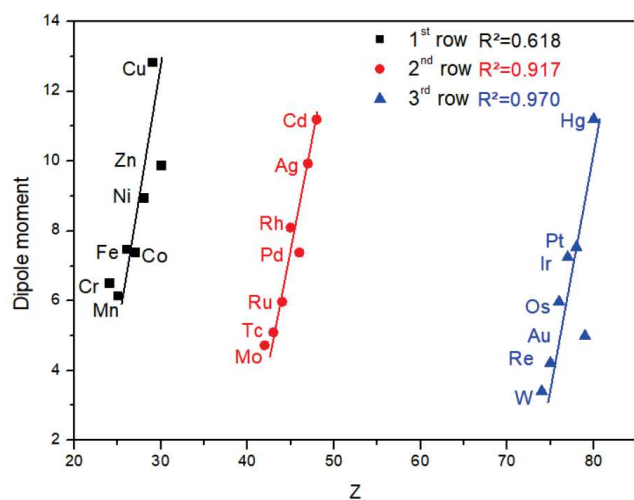


**Figure 3.** The correlation between dipole moment and atomic number of the central metal of [(bpy-CH<sub>3</sub>)M(curc)]Cl complexes for the elements of the first, second and third rows of the TMs in the periodic table. (The correlation for the 3rd row is made by excluding Au)

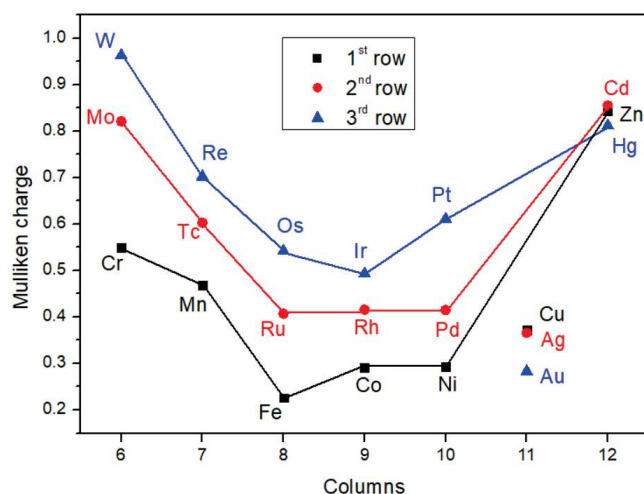




**Figure 4.** Plot of Mulliken charge of metals of [(bpy-CH<sub>3</sub>)M(curc)]Cl complexes as function of their position in the periodic table.

The plot of Mulliken charge of the metals as function of their position in the periodic table is given in Figure 4, and this variation is similar for the three rows, Cu, Ag and Au excepted, and the Mulliken charge of the TMs follows the trend: 1<sup>st</sup> row < 2<sup>nd</sup> row < 3<sup>rd</sup> row. Indeed, this feature matches what that was said above.

All complexes have a pyramidal geometry with square base, as it is illustrated in Figure S-1 in Supplementary Info, with some exceptions for:

- The column of Cr, Mo and W that shares the trigonal bipyramid geometry. Indeed, they have the same electronic configuration of the metal atoms (n-1)d<sup>5</sup>ns<sup>1</sup>, and their structures are predicted by VSEPR model so that they are characterized by AX<sub>5</sub>E<sub>0</sub> trigonal bipyramid.<sup>[52]</sup> In these bipyramids, the basal plane contains one oxygen, one nitrogen, and the chlorine.

- The same trigonal bipyramid structure is that of the Cu complex. One knows that the atomic preferred configuration of Cu is 3d<sup>10</sup>4s<sup>1</sup> and that exchanges between bipyramid and square plane pyramid are driven from a strong Jahn-Teller contribution, as explained in the detailed study of Reinen et al.<sup>[53,54]</sup>

The trigonal bipyramid geometry of the Hg complex is related to the spin-orbit interaction, as it has been shown in several complexes (see, *e.g.* refs<sup>[55-57]</sup>).

## Dipole moment

Dipole moment ( $\mu$ ) is an important tool for studying the intermolecular interactions because it reflects the molecular charge distribution. Therefore, it may be considered as a descriptor to represent the charge movement across the molecule. The high charge mobility in the system is explained by the high values of dipole moment which are at the origin of NLO properties of investigated systems (see, *e.g.*<sup>[58]</sup>).

All complexes exhibit a strong dipole moment and some trend can be observed from column 6 to column 12 (3.40 for W up to 12.83 Debye for Cd, see Figure S-2 in Supplementary Information). The highest values of  $\mu$  parameter are found to be 12.84 (D), 11.20 (D) and 11.20 (D) for Cu, Cd and Hg complexes, respectively, whereas the smallest value is found to be 3.404 (D) for W complex that has also the largest value of isotropic polarizability at  $1013 \times 10^{-23}$ esu. (see below).

## Solvent effect

The effect of solvation has been studied on the Zn complex. Both the geometric structure and the optical properties have been calculated at CPCM: B3LYP/LANL2DZ level of theory for selected solvents besides gas phase: Water, DMSO, Ethanol, Chloroform, Cyclohexane, and Benzene. The results are gathered in Table 1. Although the pyramid geometry with square base of the [(bpy-CH<sub>3</sub>)Zn(curc)] Cl complex is preserved in solution, our DFT calculations show significant effects. The Zn lying above the square plane becomes closer and closer to that plane when the solvent is more and more polar. Then, the distance varies from 0.54 Å in water to 0.62 Å in benzene and 0.70 Å in gas phase. In gas phase, the average distance of Zn to the O, N, Cl atoms is reduced thanks to a distortion of the basal plane (from 3.6 deg. to 15 deg.). The Zn-Cl bond length amounts 2.35 Å in gas phase, and it increases from apolar to polar solvents, varying from 2.40 Å in benzene to 2.45 Å in water.

Similarly, the dipole moment and energy gap are maximum in polar solvent phases, and lower for the less polar solvents, and even more for the gas phase (see Table 1).

**Table 1.** Average interatomic distances (Å) between M, Cl, N and O atoms, distance (Å) between Zn and the centroid between the oxygen and nitrogen atoms, average of angles (°), N<sub>α</sub>-N<sub>β</sub>-O<sub>β</sub>-O<sub>α</sub> torsion angle (°), energy gap (eV) and dipole moment (Debye) of [(bpy-CH<sub>3</sub>)Zn(curc)]Cl complex in gas and different solutions.

Phase	Average distance (Å)	Zn – Cnt (Å)	Zn-Cl (Å)	Average of angles (°)	N <sub>α</sub> -N <sub>β</sub> -O <sub>β</sub> -O <sub>α</sub> torsion angle (°)	Gap (eV)	Dipole moment (Debye)
Gas	2.201	0.697	2.348	105	15	2.874	9.89
Water	2.489	0.538	2.451	106.5	3.6	3.090	15.50
DMSO	2.489	0.540	2.449	106.5	3.6	3.092	15.43
Ethanol	2.488	0.544	2.446	106.4	3.6	3.095	15.28
Chloroform	2.485	0.576	2.422	106.2	3.7	3.119	13.92
Cyclohexane	2.480	0.626	2.390	105.8	6.6	3.096	12.02
Benzene	2.481	0.616	2.395	105.9	6	3.117	12.35

## Reactivity indices

The DFT provides several indices characterizing the reactivity.<sup>[42]</sup> The most used, global (*i.e.* characterizing the whole molecule) are the electronic chemical potential ( $\mu$ ) and global hardness

( $\eta$ ), which can be approximated from the frontier orbital energies HOMO and LUMO ( $\epsilon_H$  and  $\epsilon_L$  respectively). Electronic chemical potential ( $\mu$ ) is the tendency of an atom or molecule to not let escape its electrons, it is given by the following equation:

$$\mu = \frac{1}{2}(\epsilon_H + \epsilon_L) \quad (1)$$

The absolute hardness ( $\eta$ ) expresses the resistance of a system to change its number of electrons; it is given by following the equation:

$$\eta = (\epsilon_H - \epsilon_L) \quad (2)$$

The softness is just the inverse of the hardness  $S=1/\eta$ . Therefore, a good nucleophile is characterized by low value of  $\mu$ , and a good electrophile is characterized by high value of  $\mu$ .

**Table 2.** Global reactivity descriptors: chemical potential ( $\mu$ , eV), chemical hardness ( $\eta$ , eV) and electrophilicity index ( $\omega$ , eV) of [(bpy-CH<sub>3</sub>)M(curc)]Cl complexes calculated at B3LYP/LANL2DZ level.

	$\mu$	$\eta$	$\omega$
Cr	-3.327	2.056	2.691
Mn	-3.756	2.806	2.514
Fe	-3.544	2.680	2.344
Co	-3.483	2.462	2.464
Ni	-3.324	1.643	2.844
Cu	-3.832	2.674	2.745
Zn	-3.830	2.902	2.508
Mo	-3.270	1.780	3.003
Tc	-3.530	2.444	2.549
Ru	-3.444	2.495	2.376
Rh	-3.377	2.152	2.650
Pd	-3.607	1.831	3.552
Ag	-3.750	3.175	2.215
Cd	-3.842	2.753	2.680
W	-3.274	1.719	3.119
Re	-3.478	2.199	2.750
Os	-3.347	2.206	2.540
Ir	-3.306	2.111	2.588
Pt	-3.626	1.787	3.670
Au	-3.57	2.685	2.373
Hg	-3.804	2.787	2.597

Table 2 contains the computed chemical potential ( $\mu$ , eV) and chemical hardness ( $\eta$ , eV) values for the TM [(bpy-CH<sub>3</sub>)M(curc)] Cl complexes. It is important to note that the chemical potential follows the same trend that the softness by rows from the periodic table, except for the TMs from the first and second rows that share the electronic configuration (n-1)d<sup>10</sup>ns<sup>0,2</sup>. For the third

row, it is verified only for the TMs that have the electronic configuration  $5d^x6s^2$  where  $x=4,5,10$  (Figures 5 and 6 and S-3). The results of ( $\mu$ ) and ( $\eta$ ) indicate that  $[(bpy-CH_3)Ag(curc)] Cl$  is the most harder,  $[(bpy-CH_3)Cd(curc)] Cl$  is the least reactive and  $[(bpy-CH_3)Mo(curc)] Cl$  and  $[(bpy-CH_3)W(curc)] Cl$  are the most reactive.

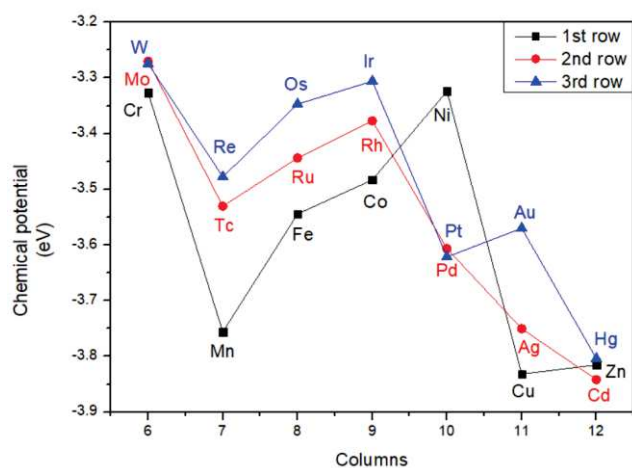


**Figure 5.** Plot of the chemical potential (eV) of  $[(bpy-CH_3)M(curc)]Cl$  complexes as function of the position of the metals in the periodic table.

The reactivity of the complexes of the TMs  $[(bpy-CH_3)M(curc)] Cl$  follows the order:

1<sup>st</sup> row: Ni > Cr > Co > Fe > Mn > Zn > Cu

2<sup>nd</sup> row: Mo > Rh > Ru > Tc > Pd > Ag > Cd

3<sup>rd</sup> row: W > Ir > Os > Re > Au > Pt > Hg

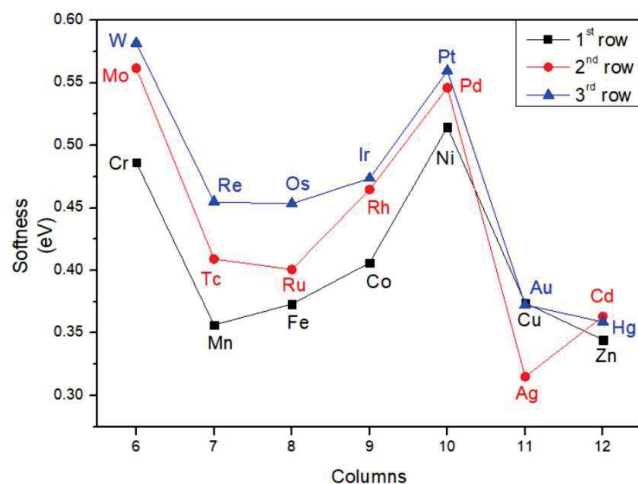


**Figure 6.** Plot of the softness (eV) of  $[(bpy-CH_3)M(curc)]Cl$  complexes as function of the position of the metals in the periodic table.

1  
2  
3  
4  
5  
6  
7  
8  
9  
10  
11  
12  
13  
14  
15  
16  
17  
18  
19  
20  
21  
22  
23  
24  
25  
26  
27  
28  
29  
30  
31  
32  
33  
34  
35  
36  
37  
38  
39  
40  
41  
42  
43  
44  
45  
46  
47  
48  
49  
50  
51  
52  
53  
54  
55  
56  
57  
58  
59  
60  
61  
62  
63  
64  
65

As shown in Figure S-3, the hardness of the TMs complexes varies in the same manner for the three rows with respect to the position of the metal in the periodic table, except for Ru et Cd, and the classification of their values follows: 1<sup>st</sup> row > 2<sup>nd</sup> row > 3<sup>rd</sup> row.

### Vibration frequencies

The calculated IR spectra of 21 optimized molecules of [(bpy-CH<sub>3</sub>)M(curc)] Cl complexes have been presented in Figure S-4. Generally, on accounting on anharmonicity and basis set deficiencies, it is known that harmonic DFT frequencies overestimate the experimental (anharmonic) vibration wavenumbers. Therefore, the calculated vibration wavenumbers have been scaled down by, in case of the B3LYP functional, a factor equal to 0.9614.<sup>[43]</sup> The spectra exhibit three bands: (a) a high frequency near 1400-1550 cm<sup>-1</sup> related to the C=O stretching, (b) an intermediate band of C-H deformation between 1100-1250 cm<sup>-1</sup> (c) a large bunch of frequencies (2900-3200 cm<sup>-1</sup>) related to CH<sub>3</sub> stretching.

The CO symmetrical stretching vibrations for Zn complex have been shifted from 1625 cm<sup>-1</sup> to 1605 cm<sup>-1</sup>.<sup>[39]</sup> The theoretical corresponding peaks are also calculated at 1490 for Zn complex and in the region of 1353-1466 cm<sup>-1</sup> for the other TMs complexes. The H-bonded enol proton stretching of [(bpy-CH<sub>3</sub>)Zn(curc)] Cl complex observed experimentally in the region of 2600-3800 cm<sup>-1</sup>, has been calculated theoretically to be 3506 cm<sup>-1</sup>.

In the following part, we propose to inspect the effect of the central metal on the frequencies of the functions. Table S-2 presents the calculated frequencies of C=O, M-O1, M-O2, M-N1 and M-N2 of the 21 TMs complexes. The frequency of C=O function increases from left to right through from the periodic table for W and Rh excepted. One has also a general decrease of the frequencies from the first row (3d) towards the third row (5d). On the whole, the C=O varies from 1353 cm<sup>-1</sup> (W) to 1466 cm<sup>-1</sup>(Cd). The M-Cl elongation has been shifted from 160 cm<sup>-1</sup> (for Pd) to 356 cm<sup>-1</sup> (for Fe). The M-O vibrations are calculated in the region of 550-588 cm<sup>-1</sup> and the M-N vibrations in the region of 504-576 cm<sup>-1</sup>.

In order to examine the solvent effect on the HOMO-LUMO energy and electronic spectrum (Table 1 and Figure 7), six different solvents (water, ethanol, DMSO, chloroform, cyclohexane and benzene) are used. The calculated IR spectra for the Zn complex at B3LYP/LANLD2Z presented in Figure 7 show an increase in the intensity of the peaks of solvated complexes compared with the results of gas phase, and the peaks found in polar solvents are more intense than those in apolar solvents, as expected.

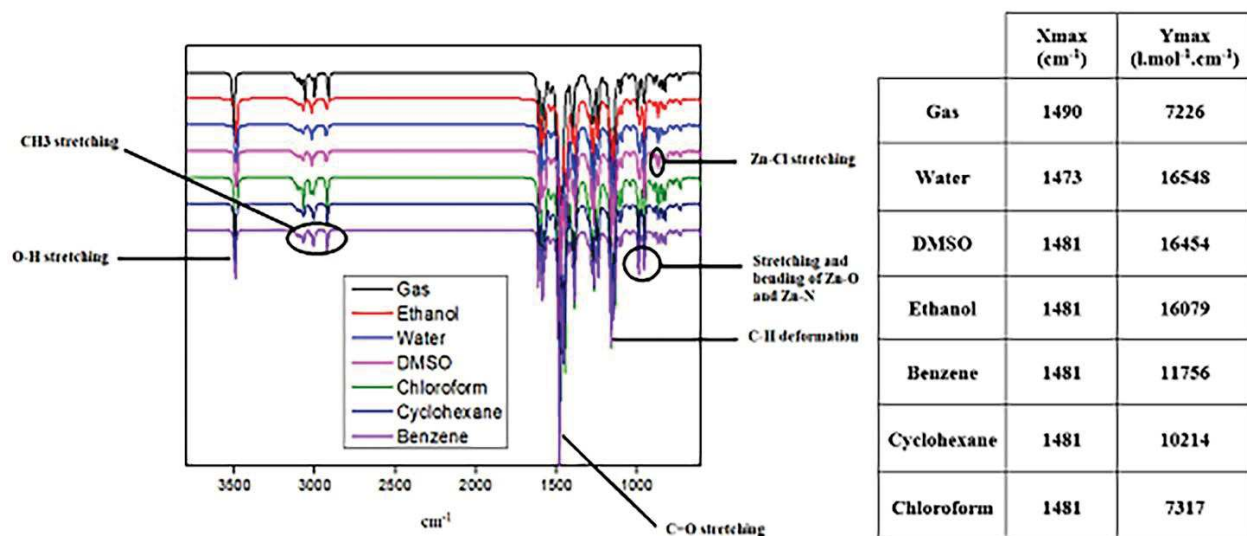


**Figure 7.** Calculated IR spectra for the Zn complex in gas and different solutions phases.

### Electronic absorption and emission spectra

For the first time, TD-DFT restricted calculations of the electronic absorption transition of [(bpy-CH<sub>3</sub>)Zn(curc)] Cl complex have been attempted. The results of the calculated electronic absorption spectrum of Zn complex recorded in gas phase at room temperature is given in Figure 8. The maximum absorption wavelength is found to be 425 nm. The experimental and theoretical emission spectra of Zn complex in DMSO are also reported in Figure 8. They give a maximum emission wavelength at 495 nm which is not far from the experimental value (543 nm).<sup>[39]</sup> A better agreement of the emission spectrum with experiment would require a choice of a more adapted functional, but the trends would not be functional dependent.

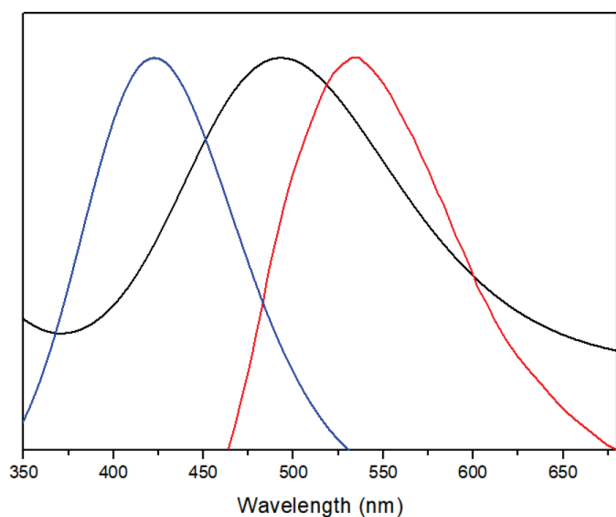


**Figure 8** Absorption and emission spectra of  $[(\text{bpy-CH}_3)\text{Zn}(\text{curc})]\text{Cl}$  complex at room temperature (Blue: Calculated absorption spectra in gas phase, Black: calculated emission spectra in DMSO, Red: experimental emission spectra in DMSO from [39])

### The influence of the nature of central metal and the solvent on the electronic spectra

For the study of the nature of frontier orbitals of TMs complexes in gas phase, Table S-3 reports the frontier orbitals of 21 complexes. As can be seen in Table S-3, the largest energy gap in each row is for Zn, Cd and Hg complexes, their central atom belonging to the periodic column 12, with their d shell filled: Accordingly, their HOMO-LUMO orbitals have a curc-curc character. For Cr, Mo and W that share the same electronic configuration according to Klechkowski's filling, their HOMO-LUMO are as byp-curc. Ir and Pt from the third row have the smallest energy gap values, and have a HOMO-LUMO of byp-byp character. The largest metal Mulliken charges in the second and third row are for Ag and Au complexes, and their frontier orbitals are in the byp-curc form.

The molecular orbital diagrams of  $[(\text{bpy-CH}_3)\text{M}(\text{curc})]\text{Cl}$  complexes where  $\text{M}=\text{Fe}, \text{Ni}, \text{Cu}$  and  $\text{Zn}$ , shows the different character of the frontier orbitals among the various complexes of the study (see Figure S-5).

**Table 3.** Absorption wavelength (nm), oscillator strengths (f), electronic transitions, contribution percentage (%), transition type, energy gap (eV) of  $[(\text{bpy-CH}_3)\text{M}(\text{curc})]\text{Cl}$  complexes where  $\text{M} = \text{Cr}, \text{Mn}, \text{Fe}, \text{Co}, \text{Ni}, \text{Cu}, \text{Zn}, \text{Mo}, \text{Tc}, \text{Ru}, \text{Rh}, \text{Pd}, \text{Ag}, \text{Cd}, \text{W}, \text{Re}, \text{Os}, \text{Ir}, \text{Pt}, \text{Au}$  and  $\text{Hg}$  calculated at B3LYP/LANL2DZ in gas phase.

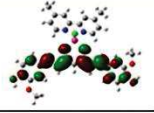
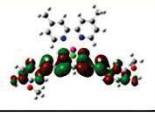
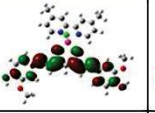
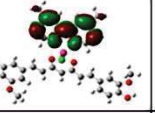
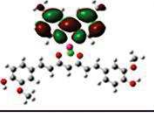
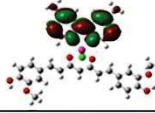
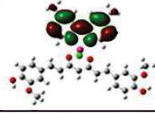
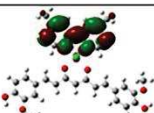
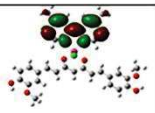
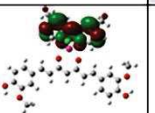
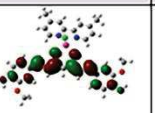
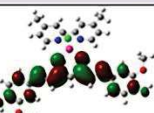
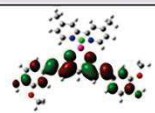
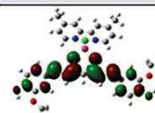
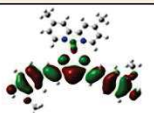
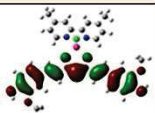
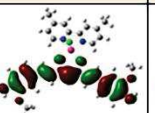
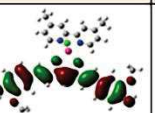
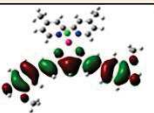
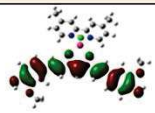
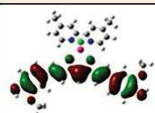
	$\lambda_{\text{abs}}$ (nm)	f	Electronic transitions	Contribution percentage (%)	Transition type	Energy gap (eV)
Cr	402	1.006	H-2 $\rightarrow$ L+1	38	LLCT	0.594
Mn	441	0.701	H-2 $\rightarrow$ L	30	LLCT	0.224
Fe	427	0.895	H-3 $\rightarrow$ L+1	45	LMCT	0.709
Co	431	0.592	H-2 $\rightarrow$ L+2	25	MLCT	0.523
Ni	437	1.105	H-3 $\rightarrow$ L	87	LLCT	0.180
Cu	429	0.569	H $\rightarrow$ L+1	26	MLCT	0.490
Zn	425	1.276	H $\rightarrow$ L+1	98	LLCT	1.942
Mo	419	1.293	H-2 $\rightarrow$ L	42	ICLT	0.884
Tc	423	0.384	H-3 $\rightarrow$ L ( $\alpha$ )	24	ICLT	0.230
			H-1 $\rightarrow$ L+5 ( $\beta$ )	34	ICLT	
Ru	426	0.694	H-3 $\rightarrow$ L+1	80	LMCT	0.150
Rh	431	0.473	H-3 $\rightarrow$ L+1	26	ICLT	0.132
Pd	446	1.147	H-3 $\rightarrow$ L	92	LMCT	0.208
Ag	421	1.276	H $\rightarrow$ L( $\alpha$ )	43	LLCT	0.779
			H $\rightarrow$ L+1( $\beta$ )	43	LLCT	
Cd	423	1.315	H $\rightarrow$ L+1	99	LLCT	1.953
W	418	0.994	H-1 $\rightarrow$ L+5	28	ICLT	0.848
Re	429	0.549	H $\rightarrow$ L+2( $\alpha$ )	21	ICLT	0.306
			H-1 $\rightarrow$ L+6( $\beta$ )	21	LLCT	
Os	414	0.547	H-1 $\rightarrow$ L+3	35	LLCT	0.302
Ir	429	0.800	H-3 $\rightarrow$ L	40	LLCT	0.153
Pt	451	0.965	H-3 $\rightarrow$ L	86	LLCT	0.185
Au	440	0.835	H-1 $\rightarrow$ L( $\alpha$ )	39	LLCT	0.604
			H $\rightarrow$ L+1( $\beta$ )	41	LLCT	
Hg	424	1.284	H $\rightarrow$ L+1	98	LLCT	1.977

Table 3 reports the result of the calculated electronic absorption of TMs complexes in gas phase. As can be seen in this Table, the position of the maximum absorption band of the title complexes depends modestly on the nature of central metal. The highest absorption wavelength lies in the 451 nm – 402 nm range. The highest values of contribution percentage on TMs complexes are: 87% for Ni, 98% for Zn, 80% for Ru, 92% for Pd, 99% for Cd, 86% for Pt and 98% for Hg, characterizing ligand to another ligand charge transfer (LLCT) from curcumin to bipyridine ligand. For the elements Mo, Tc, Rh and W, the highest values of contribution percentage of absorption maxima are characterized as intra-ligand charge transfer (ICLT) bands. Besides, Re complex exhibits combined charge transitions of ligand to same ligand (ICLT) and ligand to another ligand (LLCT) with 21% of contribution percentage.

Additionally, the UV-Vis spectrum of the Zn complex has been calculated in different solvents in order to examine the solvent effect on the electronic absorption (see Figure S-6). The Zn



complex exhibits strong absorption in the UV-Vis region. The maximum absorption in DMSO solution is found to be located at 454 nm, very close to the experimental value found in the range of 408-450 nm.<sup>[39]</sup> The HOMO→LUMO transition is the major electronic transition in polar solvents with 100% of contribution percentage, and it is characterized as intra-ligand charge transfer (ILCT). However, in cyclohexane and benzene solutions, the highest absorption wavelength comes from a HOMO → LUMO+1 contribution (100%) which corresponds to a ligand to another ligand charge transfer (LLCT). This is seen in Figure 9 where the HOMO, LUMO and LUMO+1 are depicted facing their eigenvalues and the dipole moment of the solvent. The swap between LUMO and LUMO+1 is clearly apparent as soon as the dipole exists, whereas the gaps between HOMO and LUMO (hardness) as well as LUMO and LUMO+1 remain quasi-unchanged. A rather similar solvatochromism was observed by Larsen et al. in a rhenium complex<sup>[59]</sup>: in both cases the ILCT is a shift of the density from the end of the ligand (curcumin in our case) towards the atoms (of the same ligand) linked to the metal (O here, N in<sup>[59]</sup>), although their ILCT is typically a left-right shift of the ligand density, whereas it is more end-to-center of the curcumin ligand in our case.

solvent	(gas)	Benzene	Cyclohexane	Chloroform	DMSO	Ethanol	water
Dielectric const.		2.27	2.02	4.81	46.7	24.5	80.1
Dipole moment		0	0	1.15	3.9	1.69	1.82
LUMO+1 energy	-2.091	-2.329	-2.304	-2.325	-2.332	-2.323	-2.331
							
LUMO energy	-2.393	-2.353	-2.354	-2.444	-2.564	-2.550	-2.566
							
HOMO energy	-5.267	-5.470	-5.450	-5.562	-5.655	-5.645	-5.660
							

**Figure 9.** Orbital energy level diagrams of the molecular orbitals involved (highlighted) in the excitation transitions for Zn complex obtained at B3LYP/LANL2DZ in gas and different solvent phases.

1  
2  
3  
4  
5  
6  
7  
8  
9  
10  
11  
12  
13  
14  
15  
16  
17  
18  
19  
20  
21  
22  
23  
24  
25  
26  
27  
28  
29  
30  
31  
32  
33  
34  
35  
36  
37  
38  
39  
40  
41  
42  
43  
44  
45  
46  
47  
48  
49  
50  
51  
52  
53  
54  
55  
56  
57  
58  
59  
60  
61  
62  
63  
64  
65

The determination of molecular electric transport properties, the measurement of electronic conductivity as well as the molecular chemical stability are mainly driven by the energy gap ( $\Delta E$ ). Table 3 indicates that the highest HOMO-LUMO energy gap is in Hg, Cd and Zn complexes (with values of 1.977 eV, 1.953 eV and 1.942 eV, respectively) pointing out that they are the hardest molecules. Whereas the softest ones are Rh, Ru and Ir complexes with energy gap values amounting 0.132 eV, 0.150eV and 0.153 eV, respectively. The ranking of energy gap from high to low is:

$$\Delta E_{Hg} > \Delta E_{Cd} > \Delta E_{Zn} > \Delta E_{Mo} > \Delta E_W > \Delta E_{Ag} > \Delta E_{Fe} > \Delta E_{Au} > \Delta E_{Cr} > \Delta E_{Co} > \Delta E_{Cu} > \Delta E_{Re} > \Delta E_{Os} > \Delta E_{Tc} > \Delta E_{Mn} > \Delta E_{Pd} > \Delta E_{Pt} > \Delta E_{Ni} > \Delta E_{Ir} > \Delta E_{Ru} > \Delta E_{Rh}$$

The solvent can affect, not only the equilibrium geometries of molecules but also their optical activity, as it is well known. Six solvents with different polarities, namely water, DMSO, ethanol, cyclohexane, chloroform and benzene are investigated for this purpose. The UV-Vis electronic spectrum of Zn (II) complex calculated at PCM TD-B3LYP/LANL2DZ level of theory are reported in FigureS-6. The highest wavelength absorption in DMSO solution, experimentally observed in the 408-450 nm range<sup>[39]</sup> is calculated to be near 452 nm.

As can be seen from Figure S-6, a bathochromic effect resulting from the solvent effect are clearly noted; and the decreasing classification of the maximum wavelengths of absorption is given as follows: DMSO > Water > Ethanol > Chloroform > Benzene > Cyclohexane. The absorption maxima have been found at 452 nm in water and ethanol, 454 nm in DMSO, 447 nm in cyclohexane, 451 nm in chloroform and 449 nm in benzene. These shifts are rather small, but they follow the polarity of the solvents, as expected. The ranking of the molar absorption coefficient ( $\epsilon$ ) from high to low is:

Benzene > Chloroform > Ethanol > Cyclohexane > DMSO  $\geq$  Water > Gas

### Thermodynamic parameters

The different thermodynamic parameters like zero-point vibrational energy, Gibbs free energy ( $G$ ), entropy ( $S$ ) and enthalpy ( $H$ ) play an important role in the characterization of molecular systems.

Our aim of this point is to make comparison between TMs and to yield extensive look-up characteristics of thermodynamics. The thermodynamic calculations of [(bpy-CH<sub>3</sub>)M(curc)] Cl complexes, where M = Cr, Mn, Fe, Co, Ni, Cu, Zn, Mo, Tc, Ru, Rh, Pd, Ag, Cd, W, Re, Os, Ir,

Pt, Au and Hg, have been computed in gas phase, at 298.15 K and 1 atm for the optimized structures using B3LYP/LANL2DZ levels of theory. The obtained results are presented in Table 4. By varying the central metal, the zero-point vibrational energy and thermal energy change slightly, and their values lie between 361 kcal/mol and 364 kcal/mol, and between 388 kcal/mol and 390 kcal/mol, respectively. This indicates that the vibrations of the ligands are unchanged (*i.e.* the ligand is rather rigid), and the unique change is due to the metal-ligand distances, greater as far as the cation is bigger

**Table 4.** Thermodynamic parameters of the [(bpy-CH<sub>3</sub>)M(curc)]Cl complexes.

	Thermal properties (Hartree/Particle)		S (cal/Mol- Kelvin)	Dipole moment (D)	Zero-point vibrational energy (Kelvin.cal/mol)	Total thermal energy (Kelvin.cal/Mol)	C <sub>v</sub> (cal/ Mol- Kelvin)	Rotational Constants (GHz)		
	Sum of electronic and thermal Free Energies	Sum of electronic and thermal Enthalpies						X	Y	Z
Zn	-1916.953	-1916.824	269.817	9.89	362.783	389.785	157.835	0.061	0.035	0.024
Cu	-2047.458	-2047.327	275.429	12.83	362.843	389.818	157.638	0.065	0.033	0.025
Ni	-2020.619	-2020.492	267.472	8.95	363.989	390.504	156.508	0.066	0.035	0.024
Co	-1996.419	-1996.293	265.175	7.39	364.126	390.508	156.404	0.065	0.035	0.024
Fe	-1974.765	-1974.639	265.361	7.48	364.043	390.343	156.241	0.065	0.035	0.023
Mn	-1955.254	-1955.128	265.064	6.15	363.375	389.839	156.850	0.064	0.035	0.024
Cr	-1937.628	-1937.504	260.916	6.51	363.578	389.841	156.522	0.068	0.034	0.025
Cd	-1899.403	-1899.269	282.224	11.19	361.937	389.409	158.413	0.055	0.034	0.023
Ag	-1997.012	-1996.879	280.747	9.93	361.589	389.099	158.603	0.056	0.034	0.023
Pd	-1978.016	-1977.890	266.319	7.38	363.567	390.200	157.038	0.057	0.036	0.022
Rh	-1960.825	-1960.698	268.234	8.09	363.650	390.191	156.705	0.059	0.036	0.023
Ru	-1945.201	-1945.076	236.765	5.97	363.589	389.944	156.519	0.059	0.036	0.023
Hg	-1894.032	-1893.896	285.994	11.20	361.520	389.211	158.708	0.050	0.034	0.024
Au	-1986.687	-1986.554	279.649	4.98	361.810	389.273	158.432	0.052	0.035	0.022
Pt	-1970.445	-1970.319	266.086	7.53	363.902	390.461	156.761	0.056	0.035	0.022
Ir	-1956.011	-1955.884	267.206	7.24	363.789	390.240	156.507	0.059	0.036	0.023
Os	-1942.352	-1942.226	264.676	5.97	363.385	389.720	156.551	0.059	0.035	0.023
Mo	-1918.855	-1918.730	261.656	4.72	362.717	389.055	157.151	0.067	0.033	0.025
Re	1930.408	-1930.283	263.853	4.21	362.848	389.216	157.108	0.066	0.033	0.025
Tc	-1931.393	-1931.268	263.716	5.09	363.103	389.482	156.944	0.066	0.033	0.025
W	-1919.148	-1919.024	261.032	3.40	362.437	388.742	157.383	0.067	0.033	0.025

Figure S-7 (in Supplementary Information) presents an excellent linear correlation between sum of electronic and thermal free energies and covalent radius of TMs for the columns 6, 7, 8, 9

and 10 of the periodic table. As can be seen in Figure S-7, the difference is strictly related to the smaller size of the metals of the first transition series with respect to the metals of the second and third series which are quasi-similar, thanks to the relativistic corrections in the heavy atoms (third row), as is well known.

## Nonlinear Optical Parameters

Presently, TMs materials are very interesting in the study of nonlinear optical properties (NLO), especially that they have caught the attention of many specialists in the field of novel technology developments in optics and photonics<sup>[60-65]</sup> TMs materials can be used as amplifiers,<sup>[66,67]</sup> and they are attractive in many optical applications as all-optical switching,<sup>[5,6,68,69]</sup> optical limiting<sup>[70,71]</sup> and also as optical devices.<sup>[9-11]</sup> Nonlinear optical phenomena may be produced by applying electromagnetic fields in various material systems in order to get new electromagnetic fields altered in amplitude, phase, frequency and other physical properties.<sup>[11,72]</sup> The Nonlinear optical (NLO) properties like the isotropic polarizability ( $\alpha$ ), the anisotropy of the polarizability ( $\Delta\alpha$ ) and the first order hyperpolarizability ( $\beta$ ) of the title molecules are calculated. The polarizability ( $\alpha$ ) and first hyperpolarizability ( $\beta$ ) reveals the response of a system in an applied electromagnetic field. Six components of  $\alpha_{xx}$ ,  $\alpha_{xy}$ ,  $\alpha_{yy}$ ,  $\alpha_{xz}$ ,  $\alpha_{yz}$ , and  $\alpha_{zz}$ , and ten components of  $\beta$  as  $\beta_{xxx}$ ,  $\beta_{yxx}$ ,  $\beta_{xyy}$ ,  $\beta_{yyy}$ ,  $\beta_{zxx}$ ,  $\beta_{xyz}$ ,  $\beta_{zyy}$ ,  $\beta_{xzz}$ ,  $\beta_{yzz}$  and  $\beta_{zzz}$  are provided from the Gaussian09 output file. The isotropic polarizability ( $\alpha$ ) and the anisotropy of the polarizability ( $\Delta\alpha$ ) have been computed using the following equations:

$$\alpha = \frac{1}{3}(\alpha_{xx} + \alpha_{yy} + \alpha_{zz}) \quad (3)$$

$$\Delta\alpha = \left[ \frac{(\alpha_{xx}-\alpha_{yy})^2 + (\alpha_{yy}-\alpha_{zz})^2 + (\alpha_{zz}-\alpha_{xx})^2}{2} \right]^{\frac{1}{2}} \quad (4)$$

The magnitude of the first order hyperpolarizability tensor ( $\beta$ ), using the x, y and z components are defined as:

$$\beta = \sqrt{\beta_x^2 + \beta_y^2 + \beta_z^2} \quad (5)$$

where:

$$\beta_x = \beta_{xxx} + \beta_{xyy} + \beta_{xzz} \quad (6)$$

$$\beta_y = \beta_{yyy} + \beta_{xxy} + \beta_{yyz} \quad (7)$$

$$\beta_z = \beta_{zzz} + \beta_{xxz} + \beta_{yyz} \quad (8)$$

The results of calculations in gas phase are given in Tables 5 and 6.

**Table 5.** Anisotropy of polarizability ( $\Delta\alpha$ )(esu), polarizability ( $\alpha$ )(esu)[(bpy-CH<sub>3</sub>)M(curc)]Cl complexes calculated at B3LYP/LANL2DZ in gas phase, and their components.

	$\alpha_{xx} \times 10^{-23}$	$\alpha_{xy} \times 10^{-23}$	$\alpha_{yy} \times 10^{-23}$	$\alpha_{xz} \times 10^{-23}$	$\alpha_{yz} \times 10^{-23}$	$\alpha_{zz} \times 10^{-23}$	$\alpha \times 10^{-23}$	$\Delta\alpha \times 10^{-23}$
Cr	1330.8	66.3	950.6	-51.7	26.7	481.9	921.1	736.4
Mn	1392.2	-33.7	1003.9	-37.6	-41.4	355.9	917.4	906.9
Fe	1337.9	-32.9	907	-4.2	-17.1	306.6	850.5	897.2
Co	1328.3	-44.6	849.8	-17.3	-1.9	326.2	834.8	868.1
Ni	1363.7	-33.8	858.7	14.9	-42.3	330.7	851.1	894.7
Cu	1249.1	30	715.8	-30.9	1.9	472.6	812.5	687.9
Zn	1293.8	-39.9	697.9	-39.1	21.5	352.2	781.3	824.9
Mo	1419.5	100.9	1032.3	50.9	-30.1	534.8	995.5	768.1
Tc	1359.9	110.8	937.9	35.9	1.6	551	949.4	700.8
Ru	1361.7	-20.9	1051.5	-1.6	-18.1	314	909.1	932.1
Rh	1347.1	-34.2	947.9	-1.5	-9.9	328.2	874.4	889.3
Pd	1400.3	-59.8	878.7	-3.9	11.9	344.4	874.5	914.4
Ag	1278.8	76.9	903	-41.3	33.9	391.9	857.9	771.1
Cd	1260.2	31.9	675.2	-52.4	-29.4	417.3	784.2	748.1
W	1453	111.7	1039.5	57.7	-25.6	545.1	1012.5	787.3
Re	1399.3	124.6	997.9	41.4	-0.1	560.5	985.9	726.6
Os	1412.9	-8.3	1185	-9.9	-12.2	322	973.3	996.7
Ir	1374.5	-25.1	1031.3	-2.9	-12.2	329.7	911.8	922.4
Pt	1409.3	-56.3	907.6	-3.2	15.5	347.7	888.2	919.9
Au	1293.7	4.7	841.7	-43.9	-38.8	389.3	841.6	783.3
Hg	1208.4	23.8	699.2	46.5	51	487.4	798.4	641.9

**Table 6.** First hyperpolarizability ( $\beta$ ) and their components (esu) of [(bpy-CH<sub>3</sub>)M(curc)]Cl complexes calculated at B3LYP/LANL2DZ in gas phase.

	$\beta_{xxx} \times 10^{-30}$	$\beta_{xxy} \times 10^{-30}$	$\beta_{xyy} \times 10^{-30}$	$\beta_{yyy} \times 10^{-30}$	$\beta_{xxz} \times 10^{-30}$	$\beta_{xyz} \times 10^{-30}$	$\beta_{yyz} \times 10^{-30}$	$\beta_{zzz} \times 10^{-30}$	$\beta_{yzz} \times 10^{-30}$	$\beta_{zzy} \times 10^{-30}$	$\beta \times 10^{-30}$
Cr	29.3	67.4	-3.9	-56.9	-2.4	-2.7	16.1	0.8	9.7	13.2	45.7
Mn	29.5	120.7	-21.5	61.3	-8.2	-8.9	-29.6	4.2	13.1	-11.8	111.2
Fe	27.6	72.7	-16.9	10.8	-2.3	-1.7	-12.8	0.3	1.6	-4.4	42.9
Co	25.2	75.7	-16.3	27.3	-4.1	-0.7	-9.9	0.7	4.5	-7.7	58.9
Ni	35.4	83.7	-13.8	23.8	-7.7	-1.9	-12.2	0.1	7.9	-11.8	65.1
Cu	72	-49.9	-18.7	-32.2	-4.2	-3.3	-4.4	1.8	-0.3	7.4	82.6
Zn	4.6	58.8	-6.3	9.2	5.5	0.5	-2.7	-0.6	1.9	-4.9	29.8
Mo	-21.9	-41.8	12.2	59.9	-4	-5.1	2.7	-0.8	-4.3	8.9	48.8
Tc	-51.6	-68.7	14.9	94.8	-5.7	-7.2	-6.9	-4.5	-10	11	84
Ru	30.9	71.5	-23.3	-25.8	-3.1	-1.8	-13.7	0.1	0.5	-4	25.2
Rh	33.5	80.3	-18.1	23.3	-2.8	-1.6	-10.9	0.2	1.5	-7.8	58.9
Pd	40.2	92.3	-25.6	14.5	-9.7	0.9	-1.9	-0.2	-1.9	-9.3	56.2
Ag	75.8	-57.9	-20.7	-48.7	-10.4	-2.3	-6.3	1.2	$6.1 \times 10^{-4}$	0.04	97.2
Cd	5.8	56.8	-1.9	7.3	-7.9	1.5	1.4	0.7	1.3	4.4	27.3
W	-10.4	-23.4	10.3	49.3	-4.3	-6.3	-4.3	-0.8	-2.6	5.3	41.3
Re	-36.9	-46.3	25.2	117.6	-6.6	-8.3	-11.2	-3.6	-7.2	5.5	104.1
<del>Os</del>	23.4	56.3	-25.1	-61.6	-3.5	-2.1	-12.8	0.02	-0.5	-3.8	46.5
Ir	35.512	84.870	-25.480	-17.803	-2.553	-1.763	-10.778	0.150	0.977	-6.243	31.045
Pt	42.949	97.015	-29.140	3.522	-8.996	0.465	-2.179	-0.274	-2.318	-8.732	49.849
Au	13.439	79.509	9.180	25.025	-9.960	1.998	-1.380	0.942	0.322	-0.777	54.494
Hg	-23.203	-56.323	11.004	-9.732	-5.835	0.551	0.133	-0.606	0.186	2.690	34.630

1  
2  
3  
4  
5  
6  
7  
8  
9  
10  
11  
12  
13  
14  
15  
16  
17  
18  
19  
20  
21  
22  
23  
24  
25  
26  
27  
28  
29  
30  
31  
32  
33  
34  
35  
36  
37  
38  
39  
40  
41  
42  
43  
44  
45  
46  
47  
48  
49  
50  
51  
52  
53  
54  
55  
56  
57  
58  
59  
60  
61  
62  
63  
64  
65

Figure 10 shows a good linear correlation between isotropic polarizability ( $\alpha$ ) and the atomic number of elements by rows in periodic table. It is possible to sort the [(bpy-CH<sub>3</sub>)M(curc)] Cl complexes according to the following order of decreasing the first order hyperpolarizability :

First row: Mn > Cu > Ni > Co > Cr > Fe > Zn

Second row: Ag > Tc > Rh > Pd > Mo > Cd > Ru

Third row: Re > Au > Pt > Os > W > Hg > Ir

From these results, the computed  $\beta$  values are found that for each row, the largest value is more than 3 times higher than the smallest value. Consequently, the Mn, Ag and Re complexes are the best candidates to NLO properties.

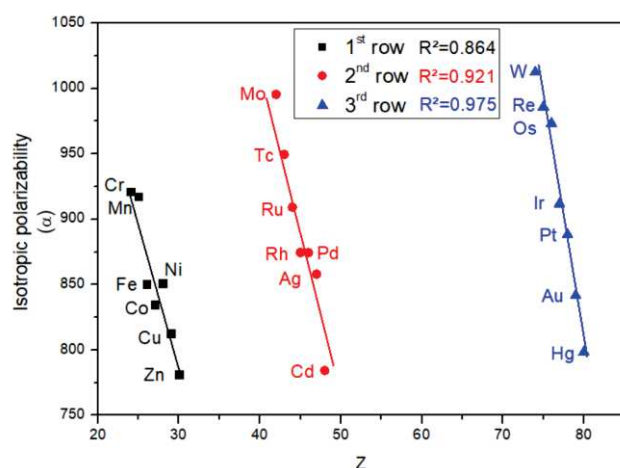


**Figure 10.** The correlation between isotropic polarizability ( $\alpha$ ) and the atomic number of elements by rows in periodic table

The magnetic moment per atom was calculated investigate the magnetic properties of the [(bpy-CH<sub>3</sub>)M(curc)] Cl complexes where M= Cr, Mn, Fe, Co, Ni, Cu, Zn, Mo, Tc, Ru, Rh, Pd, Ag, Cd, W, Re, Os, Ir, Pt, Au and Hg. The corresponding results are listed in Table 7.

**Table 7.** Magnetic moment per atom and electronic configurations of [(bpy-CH<sub>3</sub>)M(curc)]Cl complexes calculated at B3LYP/LANL2DZ in gas phase.

Magnetic moment per atom values	4.284	4.270	4.257	4.243	4.230	4.216	4.189
Element	Cu, Ag, Au,	Ni, Pd, Pt	Co, Rh, Ir	Fe, Ru, Os	Mn, Re, Tc	Cr, Mo, W	Zn, Cd, Hg
Electronic configuration	$s^1d^{10}$	$s^2d^8, d^{10}, s^1d^9$	$s^2d^7, s^1d^8$	$s^2d^6, s^1d^7$	$s^2d^5$	$s^2d^4, s^2d^4$	$s^2d^{10}$

The complexes of TMs are classified according to their magnetic moment per atom as follows:

Cu =Ag=Au > Ni=Pt=Pt > Co=Rh=Ir > Fe=Ru=Os > Mn=Re=Tc > Cr=Mo=W > Zn=Cd=Hg

As expected, there is an excellent correlation between the magnetic moments per atom and the number of valence electron of the central metals, of which they increase in the same direction. Except for the TMs, that have totally filled d and s shells, they exhibit the smallest values. The results presented in Figure 11 confirm that there is a good correlation between magnetic moment per atom and the sum of electronic and thermal free energies of the title compounds. For each periodic table row, the correlation coefficient values are  $R^2=0.966$ ,  $0.980$ ,  $0.996$  respectively. It is important to note that Zn, Cd and Hg are totally off the trend and take the smallest values of magnetic moment per atom. This result is in good agreement with the study of Mahmood et al.<sup>[73]</sup>, who showed that the value of the magnetic moment is reduced due to the strong p-d mixing between metals (Zn, Cd and Hg) and oxygen and nitrogen orbitals.

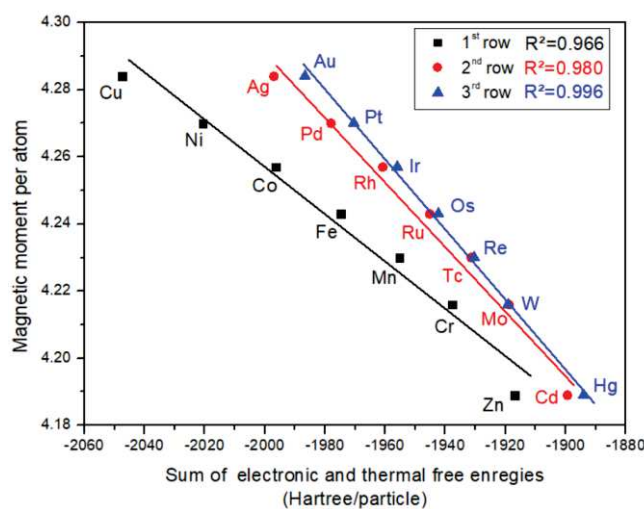


**Figure 11** Plot of the Sum of electronic and thermal free energies (Hartree/particle) as function of magnetic moment per atom of  $[(bpy-CH_3)M(curc)]Cl$  complexes in gas phase.

## Conclusion

In present work,  $[(bpy-CH_3)M(curc)] Cl$  TMs complexes were modeled by using B3LYP/LANL2DZ level to understand and clarify their geometries, electronic, thermodynamic, optical and nonlinear optical properties and to find correlation between these parameters. The DFT calculation shows that all the  $[(bpy-CH_3)M(curc)] Cl$  complexes have a



1 pyramid geometry with square base except for metals from the column with atomic electronic  
2 configuration  $n-1d^5ns^1$  and for Cu and Hg that have the largest values of the dipole moment.  
3 These last complexes share trigonal bipyramid geometry.  
4  
5

6 A good linear correlation has been found between Mulliken charge and Pauling  
7 electronegativity and atomic number of the central metal within each column from the periodic  
8 table.  
9  
10

11 The TD-DFT calculation provides an assignment of the nature of the electronic transition  
12 (LLCT, ICLT, LMCT, MLCT) in the TMs complexes in gas phase and six different solvents.  
13 Additionally, the results of thermodynamic parameter indicate an excellent linear correlation  
14 between sum of electronic and thermal free energies and covalent radius of TMs through  
15 periodic table columns, with the exception of elements which have a saturated electronic d shell  
16 with half or totally filled s shell in their valence shell.  
17  
18  
19  
20  
21  
22  
23

24 Among the curcumin complexes, the nonlinear optical properties indicate that the Mn, Ag and  
25 Re complexes are the best candidates to NLO materials. Moreover, our results show a good  
26 linear correlation between isotropic polarizability ( $\alpha$ ) and the atomic number of elements by  
27 rows in periodic table. Our results for magnetic moment per atom calculations indicate an  
28 excellent correlation with electronic configuration of central metal, knowing that the elements  
29 that have d and s shells totally filled takes the smallest values. Further, our results show an  
30 excellent correlation between magnetic moment per atom and the Sum of electronic and thermal  
31 free energies by periodic table rows.  
32  
33  
34  
35  
36  
37  
38  
39  
40  
41  
42

### 43 **Supporting Information Summary:**

44 SI contains for [(bpy-CH<sub>3</sub>)M(curc)]Cl complexes: - Some interatomic distances and angles, -  
45 Geometries, - Dipole moments, - Hardness, IR spectra, - Selected vibration frequencies, -  
46 frontier orbitals, - Absorption spectra of [(bpy-CH<sub>3</sub>)Zn(curc)]Cl in gas and different solvents,  
47 - Sum of electronic and thermal free energies as function of covalent radius of transition  
48 metals.  
49  
50  
51  
52

#### 53 **ORCID:**

54 Ahlem KHIREDDINE: 0000-0002-2524-2693  
55 Mebarek BOUKELKOUL: 0000-0002-1516-744X  
56 Yusuf ATALAY: 0000-0001-8578-5801  
57 Ömer TAMER: 0000-0002-2241-789X  
58  
59  
60  
61  
62  
63  
64  
65

1 Davut AVCI: 0000-0002-9011-6191  
2 Lynda MERZOUD: 0000-0002-6003-8882  
3 Henry CHERMETTE: 0000-0002-5890-7479  
4  
5

## 6 **Acknowledgments**

7  
8  
9 M. B and A. K. gratefully acknowledge the General Directorate of Scientific Research and  
10 Technological Development (DGRSDT) for its sponsoring. The authors gratefully  
11 acknowledge the GENCI/ CINES for HPC resources/computer time (Project cpt2130), and the  
12 PSMN of the ENS-Lyon for computing resources.  
13  
14  
15

16  
17 **Key words:** Curcumin, density functional calculations, DFT, NLO properties, quantum  
18 chemistry, thermodynamics, transition metals.  
19  
20  
21  
22  
23

## 24 **References**

- 25  
26  
27 [1] D. F. Eaton, *Science*, **1991**, *253*, 281–287.  
28  
29 [2] M. G. Papadopoulos, A. J. Sadlej, J. Leszczynski, *Non-Linear Optical Properties of Matter*,  
30 Springer, Dordrecht, **2006**.  
31  
32 [3] N. Günay, Ö. Tamer, D. Kuzaliç, D. Avci, Y. Atalay, *Opt.* **2016**, *127*, 8782–8794.  
33  
34 [4] D. Avci, A. Baçoğlu, Y. Atalay, *Struct. Chem.* **2010**, *21*, 213–219.  
35  
36 [5] G. Deng, H. Huang, C. Peng, A. Zhang, M. Zhang, S. Bo, X. Liu, Z. Zhen, L. Qiu, *RSC Adv.* **2014**, *4*,  
37 4395–4402.  
38  
39 [6] A. B. Tathe, N. Sekar, *Opt. Mater.* **2016**, *51*, 121–127.  
40  
41 [7] D. S. Chemla, J. Zyss, *Nonlinear Optical Properties of Organic Molecules and Crystals*,  
42 Academic P, New York, **1987**.  
43  
44 [8] C. Bosshard, K. Sutter, P. Prêtre, J. Hulliger, M. Flörsheimer, P. Kaatz, P. Günter, *Organic*  
45 *Nonlinear Optical Materials, Advances in Nonlinear Optics Series, Vol. 1*, Gordon & Breach,  
46 Basel, **1995**.  
47  
48 [9] K. G. Thorat, N. Sekar, *J. Photochem. Photobiol. A Chem.* **2017**, *333*, 1–17.  
49  
50 [10] A. J. Garza, O. I. Osman, N. A. Wazzan, S. B. Khan, A. M. Asiri, G. E. Scuseria, *Theor. Chem. Acc.*  
51 **2014**, *133*, 1–8.  
52  
53 [11] M. Nakano, H. Fujita, M. Takahata, K. Yamaguchi, *J. Am. Chem. Soc.* **2002**, *124*, 9648–9655.  
54  
55 [12] D. R. Kanis, M. A. Ratner, T. J. Marks, *Chem. Rev.* **1994**, *94*, 195–242.  
56  
57 [13] J.M.Hales, J. Matichak, S.Barlow, S. Ohira, K. Yesudas, J.-L. Bre'das, J. W. Perry, S. R. Marden,  
58 *Science*, **2010**, *327*, 1485–1488.  
59  
60  
61  
62  
63  
64  
65

- 1  
2  
3  
4  
5  
6  
7  
8  
9  
10  
11  
12  
13  
14  
15  
16  
17  
18  
19  
20  
21  
22  
23  
24  
25  
26  
27  
28  
29  
30  
31  
32  
33  
34  
35  
36  
37  
38  
39  
40  
41  
42  
43  
44  
45  
46  
47  
48  
49  
50  
51  
52  
53  
54  
55  
56  
57  
58  
59  
60  
61  
62  
63  
64  
65
- [14] N. B. Teran, G. S. He, A. Baev, Y. Shi, M. T. Swihart, P. N. Prasad, T. J. Marks, J. R. Reynolds, *J. Am. Chem. Soc.* **2016**, *138*, 6975.
- [15] J. L. S. Zhao, L. Kang, Y. Shen, X. Wang, M. A. Asghar, Z. Lin, Y. Xu, S. Zeng, M. Hong, *J. Am. Chem. Soc.* **2016**, *138*, 2961.
- [16] G. Maroulis, T. Bancewicz, B. Champagne, *Atomic and Molecular Nonlinear Optics: Theory, Experiment and Computation*, IOSPress, Amsterdam, **2011**.
- [17] E. Ishow, C. Bellaïche, L. Bouteiller, K. Nakatani, J. A. Delaire, *J. Am. Chem. Soc.* **2003**, *125*, 15744–15745.
- [18] P. N. Prasad, D. J. Williams, *Introduction to Nonlinear Optical Effects In Molecules and Polymers*, Vol 1, John Wiley, New York, **1991**.
- [19] J. Zyss, *Molecular Nonlinear Optics*, Elsevier, **1994**.
- [20] R. R. Tykwinski, U. Gubler, R. E. Martin, F. Diederich, C. Bosshard, P. Günter, *J. Phys. Chem. B* **1998**, *102*, 4451–4465.
- [21] Y. Q. Shi, C. Zhang, H. Zhang, J. H. Bechtel, B. H. Robinson, W. H. Steier, *Science*, **2000**, *288*, 119–122.
- [22] M. Lee, H. E. Katz, C. Erben, D. M. Gill, P. Gopalan, J. D. Heber, D. J. McGee, *Science*, **2002**, *298*, 1401–1403.
- [23] A. Goel, A. B. Kunnumakkara, B. B. Aggarwal, *Biochem. Pharmacol.* **2008**, *75*, 787–809.
- [24] S. Zorofchian Moghadamtousi, H. Abdul Kadir, P. Hassandarvish, H. Tajik, S. Abubakar, K. Zandi, *Biomed Res. Int.* **2014**, *2014*, 1–12.
- [25] M. N. Sreejayan Rao, *J. Pharm. Pharmacol.* **1997**, *49*, 105–107.
- [26] D. Vitali, P. Bagri, J. M. Wessels, M. Arora, R. Ganugula, A. Parikh, T. Mandur, A. Felker, S. Garg, M. N. V. R. Kumar, C. Kaushic, *Int. J. Mol. Sci.* **2020**, *21*, 337.
- [27] A. Gurib-Fakim, *Novel Plant Bioresources: Applications in Food, Medicine and Cosmetics*, John Wiley, Chichester, **2014**.
- [28] R. R. Mallah, D. R. Mohbiya, M. C. Sreenath, S. Chitrambalam, I. H. Joe, N. Sekar, *Opt. Mater.* **2018**, *84*, 786–794.
- [29] J. Zyss, D. Chemla, *Journal de Physique*, **1987**, 23-191.
- [30] J. L. Oudar, *J. Chem. Phys.* **1977**, *67*, 446–457.
- [31] L. R. Dalton, A. W. Harper, R. Ghosn, W. H. Steier, M. Ziari, H. Fetterman, Y. Shi, R. V. Mustacich, A. K. Y. Jen, K. J. Shea, *J. Chem. Mater.* **1995**, *7*, 1060.
- [32] M. J. Cho, D. H. Choi, P. A. Sullivan, A. J. P. Akelaitis, L. R. Dalton, *Prog. Polym. Sci.* **2008**, *33*, 1013–1058.
- [33] B. Kulyk, S. Taboukhat, H. Akdas-Kilig, J.-L. Fillaut, M. Karpierz, B. Sahraoui, *Dye. Pigment.* **2017**, *137*, 507–511.
- [34] D. J. Williams, *Angew. Chemie Int. Ed. English* **1984**, *23*, 690–703.

- 1  
2  
3  
4  
5  
6  
7  
8  
9  
10  
11  
12  
13  
14  
15  
16  
17  
18  
19  
20  
21  
22  
23  
24  
25  
26  
27  
28  
29  
30  
31  
32  
33  
34  
35  
36  
37  
38  
39  
40  
41  
42  
43  
44  
45  
46  
47  
48  
49  
50  
51  
52  
53  
54  
55  
56  
57  
58  
59  
60  
61  
62  
63  
64  
65
- [35] C. R. Moylan, *J. Phys. Chem.* **1994**, *98*, 13513–13516.
- [36] B. J. Coe, G. Chadwick, S. Houbrechts, A. Persoons, *J. Chem. Soc. Dalton Trans* **1997**, *0*, 1705.
- [37] A. Vlček, *Coord. Chem. Rev.* **2000**, *200–202*, 933–977.
- [38] A. Vlček, S. Záliš, *Coord. Chem. Rev.* **2007**, *251*, 258–287.
- [39] D. Pucci, T. Bellini, A. Crispini, I. D’Agnano, P. F. Liguori, P. Garcia-Orduña, S. Pirillo, A. Valentini, G. Zanchetta, *Medchemcomm* **2012**, *3*, 462–468.
- [40] A. Garufi, D. Trisciuglio, M. Porru, C. Leonetti, A. Stoppacciaro, V. D’Orazi, M. L. Avantageggiati, A. Crispini, D. Pucci, G. D’Orazi, *J. Exp. Clin. Cancer Res.* **2013**, *32*, 1.
- [41] G. M. Sheldrick, *Acta Crystallogr. Sect. A Found. Crystallogr.* **2008**, *64*, 112–122.
- [42] H. Chermette, *Coord. Chem. Rev.* **1998**, *178–180*, 699–721.
- [43] J. B. Foresman, Æ. Frisch, *Exploring Chemistry with Electronic Structure Methods: A Guide to Using Gaussian*, Pittsburg, **1996**.
- [44] V. Barone, M. Cossi, *J. Phys. Chem. A* **1998**, *102*, 1995–2001.
- [45] M. Cossi, N. Rega, G. Scalmani, V. Barone, *J. Comput. Chem.* **2003**, *24*, 669–681.
- [46] G. Scalmani, M. J. Frisch, *J. Chem. Phys.* **2010**, *132*, 114110.
- [47] J. P. Mészáros, J. M. Poljarevic, G. T. Gál, N. V. May, G. Spengler, É. A. Enyedy, *J. Inorg. Biochem.* **2019**, *195*, 91.
- [48] S. Das T. Saha, S. Singhan S. Kumar, *J. Mol. Struct.* **2020**, *1221*, 128732.
- [49] K. Ohwada, *Polyhedron* **1983**, *2*, 423–424.
- [50] K. Ohwada, *Polyhedron* **1984**, *3*, 853–859.
- [51] S. C. Rasmussen, *ChemTexts* **2015**, *1*, 1–9.
- [52] R. J. Gillespie, *Coord. Chem. Rev.* **2008**, *252*, 1315–1327.
- [53] D. Reinen, M. Atanasov, *Chem. Phys.* **1989**, *136*, 27–46.
- [54] R. Åkesson, L. G. M. Pettersson, M. Sandström, U. Wahlgren, *J. Am. Chem. Soc.* **1994**, *116*, 8691.
- [55] Z. Tian, D. Sander, J. Kirschner, *Phys. Rev. B - Condens. Matter Mater. Phys.* **2009**, *79*, 1–11.
- [56] C. Gourlaouen, J. P. Piquemal, T. Saue, O. Parisel, *J. Comput. Chem.* **2006**, *27*, 142–165.
- [57] R. D. Hancock, *Chem. Soc. Rev.* **2013**, *42*, 1500–1524.
- [58] M. Zaidi, D. Hannachi, H. Chermette, *Inorg. Chem.* **2021**, *60*, 6616–6632.
- [59] C. B. Larsen, H. van der Salm, C. A. Clark, A. B. S. Elliott, M. G. Fraser, R. Horvath, N. T. Lucas, X.-Z. Sun, M. W. George, K. C. Gordon, *Inorg. Chem.* **2014**, *53*, 1339–1354.
- [60] R. G. Mohamed, F. M. Elantabli, A. A. Abdel Aziz, H. Moustafa, S. M. El-Medani, *J. Mol. Struct.* **2019**, *1176*, 501–514.

- 1  
2  
3  
4  
5  
6  
7  
8  
9  
10  
11  
12  
13  
14  
15  
16  
17  
18  
19  
20  
21  
22  
23  
24  
25  
26  
27  
28  
29  
30  
31  
32  
33  
34  
35  
36  
37  
38  
39  
40  
41  
42  
43  
44  
45  
46  
47  
48  
49  
50  
51  
52  
53  
54  
55  
56  
57  
58  
59  
60  
61  
62  
63  
64  
65
- [61] M. B. . Shakerzadeh, M. Youcefizadeh, *Inorg. Chem. Commun.* **2020**, *112*, 107692.
- [62] X. Li, H. Q. Wang, J. T. Ye, Y. Zhang, Y. Q. Qiu, *J. Mol. Graph. Model.* **2019**, *89*, 131–138.
- [63] A. A. Abdel Aziz, F. M. Elantabli, H. Moustafa, S. M. El-Medani, *J. Mol. Struct.* **2017**, *1141*, 563–576.
- [64] M. Homocianu, A. Airinei, C. Hamciuc, A. M. Ipate, *J. Mol. Liq.* **2019**, *281*, 141–149.
- [65] D. Avci, S. Altürk, F. Sönmez, Ö. Tamer, A. Başoğlu, Y. Atalay, B. Z. Kurt, N. Dege, *J. Mol. Struct.* **2019**, *1197*, 645–655.
- [66] J. D. Franson, R. A. Brewster, *Phys. Lett. Sect. A Gen. At. Solid State Phys.* **2018**, *382*, 887–893.
- [67] L. Ma, Y. Tan, F. Chen, *Opt. Mater.* **2017**, *69*, 115–118.
- [68] T. Zhou, H. Jia, *Opt. Commun.* **2018**, *413*, 230–235.
- [69] S. Korposh, S. James, M. Partridge, M. Sichka, R. Tatam, *Opt. Laser Technol.* **2018**, *101*, 162–171.
- [70] M. Ramya, T. Nideep, K. Vijesh, V. Nampoore, M. Kailasnath, *Opt. Mater.* **2018**, *81*, 30.
- [71] A. F. Abdulkader, Q. M. A. Hassan, A. S. Al-Asadi, H. Bakr, H. Sultan, C. A. Emsary, *Opt.* **2018**, *160*, 100.
- [72] Y. R. Shen, *The Principles of Nonlinear Optics*, John Wiley, New York, **1984**.
- [73] Q. Mahmood, M. Hassan, S. H. A. Ahmad, K. C. Bhamu, A. Mahmood, S. M. Ramay, *J. Phys. Chem. Solids* **2019**, *128*, 283–290.

1  
2  
3  
4  
5  
6  
7  
8  
9  
10  
11  
12  
13  
14  
15  
16  
17  
18  
19  
20  
21  
22  
23  
24  
25  
26  
27  
28  
29  
30  
31  
32  
33  
34  
35  
36  
37  
38  
39  
40  
41  
42  
43  
44  
45  
46  
47  
48  
49  
50  
51  
52  
53  
54  
55  
56  
57  
58  
59  
60  
61  
62  
63  
64  
65

## Table of Contents

### DFT and TD-DFT study of curcumin complexes based on transition metals

Most complexes have a pyramidal geometry with a square base. The isotropic polarizability correlates well with the atomic number, and, among the investigated metals, the Mn, Ag and Re complexes are the best candidates to NLO materials. A good linear correlation between the magnetic moment per atom and the number of valence electron of the central metal is obtained. On the other hand, the Mulliken charge correlates well with the Pauling electronegativity and the atomic number of the transition metal.

